Metallaborane Chemistry. Part 13.[1] Direct Insertion of a Platinum Nucleophile into *nido*-5,6-$C_2B_8H_{12}$: Synthesis and Structural Elucidation of [9-H-9,9-$(Et_3P)_2$-$\mu_{10,11}$-H-7,8,9-$C_2PtB_8H_{10}$] and [9-H-9,10-$(Et_3P)_2$-7,8,9-$C_2PtB_8H_9$] *

Geoffrey K. Barker, Michael Green, F. Gordon A. Stone, and Wayne C. Wolsey
Department of Inorganic Chemistry, The University, Bristol BS8 1TS
Alan J. Welch
Dewar Crystallographic Laboratory, Department of Chemistry, University of Edinburgh, Edinburgh EH9 3JJ

The reaction (room temperature, diethyl ether) of [$Pt_2(\mu$-cod)$(PEt_3)_4$] (cod = cyclo-octa-1,5-diene) with *nido*-5,6-$C_2B_8H_{12}$ affords [9-H-9,9-$(Et_3P)_2$-$\mu_{10,11}$-H-7,8,9-$C_2PtB_8H_{10}$] (1), structurally characterised by *X*-ray diffraction. Crystals are orthorhombic, space group $P2_12_12_1$, with four molecules in a unit cell of dimensions a = 14.825(4), b = 10.1367(13), and c = 16.1193(15) Å. Using 3 303 amplitudes recorded at 293 K the structure has been refined to R = 0.0575 (R' = 0.0611). The cage of (1) approximates to a *nido*-icosahedron with a CCPtBB open face. Presumably the B–B connectivity in this face is hydrogen-bridged, but the bridge atom was not located in the crystallographic study. Thermolysis of (1) (100 °C, toluene) releases one mol equiv. of H_2 affording [9-H-9,10-$(Et_3P)_2$-7,8,9-$C_2PtB_8H_9$] (2), in which μ-H is lost and phosphine transfer from Pt to an adjacent facial B has occurred. Crystals are monoclinic, space group $P2_1/c$, with a = 9.7813(16), b = 12.312(3), c = 20.519(3) Å, β = 99.053(16)°, and Z = 4. The structure was refined to R = 0.0578 (R' = 0.0552) for 3 194 data measured at 293 K. The polyhedron of (2), formally a Pt^{II} species, shows distortion towards a closed octadecahedral architecture. The mechanism of the transformation of (1) into (2) is discussed in relation to the influence of the stereochemical changes involved.

The synthesis of carbametallaboranes by direct insertion [2] of nucleophilic metal species is now firmly established as a facile, high-yield route into an area of chemistry involving compounds which often demonstrate intriguing structure–bonding relationships,[3] and occasionally show catalytic potential.[4] In our program of synthetic and structural studies on carbametallaboranes produced by direct insertion, we herein describe results of (*i*) the reaction between [$Pt_2(\mu$-cod)$(PEt_3)_4$] [5] (cod = cyclo-octa-1,5-diene) and *nido*-5,6-$C_2B_8H_{12}$ and (*ii*) thermolysis of the compound produced therein. A preliminary account of this work has already appeared.[6]

Results and Discussion

As described in the Experimental section, [$Pt_2(\mu$-cod)$(PEt_3)_4$], a source of the highly nucleophilic $Pt(PEt_3)_2$ fragment, reacts smoothly with *nido*-5,6-$C_2B_8H_{12}$ in diethyl ether to afford in good yield a single pale yellow product (1), formulated as [$(Et_3P)_2PtC_2B_8H_{12}$]. A strong i.r. stretching frequency at 2 010 cm^{-1} was indicative of a terminal Pt–H bond, and the ^{31}P n.m.r. spectrum showed two inequivalent, but metal-bonded, phosphine ligands.

In anticipation that (1) adopts a *nido* polyhedral structure that could be closed pyrolytically, by analogy with our previous work [5,7] with [$Pt_2(\mu$-cod)$(PEt_3)_4$] and *nido*-2,3-$C_2B_4H_4R_2$ (R = H or Me), a toluene solution of (1) was heated for 1 h at 100 °C, affording one mol equiv. of gas (presumably H_2) and a red compound [$(Et_3P)_2PtC_2B_8H_{10}$] (2). The latter had spectroscopic properties very different from those of the previously characterised analogue [8,8-$(Me_3P)_2$-7,8,10-$CPtCB_8H_{10}$] [8] in that its i.r. and n.m.r. spectra showed the presence of a Pt–H group. Moreover, the ^{31}P-{^1H} n.m.r. spectrum revealed two signals at δ 17.2 and 9.6 p.p.m., with J(PtP) 2 775 and 95 Hz, respectively. The small ^{195}Pt–^{31}P coupling on the resonance at 9.6 p.p.m. established that one PEt_3 group was not bound to platinum. The thermolysis reaction had clearly proceeded in an unexpected manner, and hence the molecular structures of compounds (1) and (2) were established unequivocally by single-crystal *X*-ray diffraction.

Figures 1 and 2 give perspective views of the two molecules with the atomic numbering schemes. In Figure 2 cage hydrogen atoms take the same number as the borons or carbons to which they are attached. It was not possible in either study directly to locate the hydrido-ligand. This atom was set in an idealized position (Pt–H 1.50 Å), and in the case of (1) this represents the third *fac* site of the $PtH(PEt_3)_2$ co-ordination hemisphere, whilst for (2) the calculated hydrido-position is *cis* to P(1) and approximately *trans* to the B(4)–C(8) connectivity. Only for compound (2) were terminal hydrogen atoms of the cage located and positionally refined.

These synthetic and structural studies establish that (1) is [9-H-9,9-$(Et_3P)_2$-$\mu_{10,11}$-H-7,8,9-$C_2PtB_8H_{10}$] and that (2) is [9-H-9,10-$(Et_3P)_2$-7,8,9-$C_2PtB_8H_9$], *i.e.* that the net changes involved in thermolytic generation of (2) from (1) are loss of one mol equiv. of H_2 and transfer of a PEt_3 ligand from Pt(9) to B(10). The production of (1) from *nido*-5,6-$C_2B_8H_{12}$ and [$Pt_2(\mu$-cod)$(PEt_3)_4$], and close consideration of its pyrolytic transformation into (2), are both of interest and are discussed below. However, an important preliminary to that discussion is the following detailed comparison of the structures of the two compounds.

In Table 1 we list polyhedral bond lengths and interbond

* 10,11-μ-Hydrido-9-hydrido-9,9-bis(triethylphosphine)-7,8-dicarba-9-platinaundecaborane and 9-hydrido-9,10-bis(triethylphosphine)-7,8-dicarba-9-platinaundecaborane.

Supplementary data available (No. SUP 23649, 96 pp.): views of (1) and (2) projected onto the (0 1 0) and (1 0 0) crystal faces respectively, angles involving cage H atoms for (2), data concerning idealised H atoms, thermal parameters, observed and calculated structure factors. See Notices to Authors No. 7, *J. Chem. Soc., Dalton Trans.*, 1981, Index issue.

Table 1. Deltahedral distances (Å) and angles (°) within the compounds [9-H-9,9-$(Et_3P)_2$-$\mu_{10,11}$-H-7,8,9-$C_2PtB_8H_{10}$] (1) and [9-H-9,10-$(Et_3P)_2$-7,8,9-$C_2PtB_8H_9$] (2)

Dimension	Compound (1)	Compound (2)	Dimension	Compound (1)	Compound (2)
B(1)–B(2)	1.76(2)	1.817(18)	B(1)–B(3)–B(2)	60.6(11)	62.7(7)
B(1)–B(3)	1.74(3)	1.748(16)	B(2)–B(3)–C(7)	58.7(12)	58.8(7)
B(1)–B(4)	1.74(3)	1.797(17)	C(7)–B(3)–C(8)	54.6(8)	51.8(6)
B(1)–B(5)	1.78(2)	1.790(17)	C(8)–B(3)–B(4)	58.0(8)	54.3(6)
B(1)–B(6)	1.78(3)	1.767(15)	B(4)–B(3)–B(1)	59.5(10)	61.1(7)
B(2)–B(3)	1.74(3)	1.744(19)	B(1)–B(4)–B(3)	59.5(10)	58.4(7)
B(2)–C(7)	1.71(3)	1.682(14)	B(3)–B(4)–C(8)	59.6(9)	59.4(7)
B(2)–B(11)	1.82(3)	1.752(18)	C(8)–B(4)–Pt(9)	65.1(6)	66.5(6)
B(2)–B(6)	1.74(3)	1.725(16)	Pt(9)–B(4)–B(5)	64.7(7)	65.8(5)
B(3)–C(7)	1.76(2)	1.677(16)	B(5)–B(4)–B(1)	59.7(10)	57.9(6)
B(3)–C(8)	1.72(2)	1.679(16)	B(1)–B(5)–B(4)	57.8(10)	58.3(6)
B(3)–B(4)	1.77(2)	1.788(18)	B(4)–B(5)–Pt(9)	66.1(8)	64.2(5)
B(4)–C(8)	1.69(2)	1.584(15)	Pt(9)–B(5)–B(10)	71.3(8)	64.6(5)
B(4)–Pt(9)	2.208(15)	2.229(12)	B(10)–B(5)–B(6)	58.8(9)	59.8(6)
B(4)–B(5)	1.83(3)	1.897(15)	B(6)–B(5)–B(1)	59.5(10)	59.2(6)
B(5)–Pt(9)	2.184(18)	2.259(10)	B(1)–B(6)–B(2)	59.8(11)	62.7(7)
B(5)–B(10)	1.73(2)	1.719(15)	B(2)–B(6)–B(11)	62.3(11)	60.0(7)
B(5)–B(6)	1.81(2)	1.788(16)	B(11)–B(6)–B(10)	61.9(10)	56.4(6)
B(6)–B(10)	1.74(2)	1.748(14)	B(10)–B(6)–B(5)	58.5(9)	58.2(6)
B(6)–B(11)	1.77(3)	1.778(15)	B(5)–B(6)–B(1)	59.3(9)	60.5(7)
C(7)–C(8)	1.60(2)	1.466(15)	B(11)–C(7)–B(2)	65.2(12)	62.2(7)
C(8)–Pt(9)	2.143(10)	2.159(10)	B(2)–C(7)–B(3)	60.1(11)	62.6(7)
Pt(9)–B(10)	2.313(14)	2.175(10)	B(3)–C(7)–C(8)	61.6(10)	64.1(8)
B(10)–B(11)	1.81(2)	1.667(16)	C(7)–C(8)–B(3)	63.8(10)	64.1(7)
B(11)–C(7)	1.67(3)	1.708(16)	B(3)–C(8)–B(4)	62.4(9)	66.4(7)
			B(4)–C(8)–Pt(9)	69.1(6)	71.2(6)
B(2)–B(1)–B(3)	59.6(12)	58.5(7)	C(8)–Pt(9)–B(4)	45.8(6)	42.3(4)
B(3)–B(1)–B(4)	61.1(11)	60.6(7)	B(4)–Pt(9)–B(5)	49.1(7)	50.0(4)
B(4)–B(1)–B(5)	62.6(9)	63.8(7)	B(5)–Pt(9)–B(10)	45.3(6)	45.6(4)
B(5)–B(1)–B(6)	61.2(9)	60.3(6)	Pt(9)–B(10)–B(5)	63.4(7)	69.8(5)
B(6)–B(1)–B(2)	59.1(11)	57.5(7)	B(5)–B(10)–B(6)	62.7(10)	62.1(7)
B(1)–B(2)–B(3)	59.8(11)	58.7(7)	B(6)–B(10)–B(11)	60.0(10)	62.7(6)
B(3)–B(2)–C(7)	61.3(11)	58.6(7)	B(10)–B(11)–B(6)	58.2(9)	60.9(6)
C(7)–B(2)–B(11)	56.1(10)	59.6(7)	B(6)–B(11)–B(2)	58.0(11)	58.5(6)
B(11)–B(2)–B(6)	59.6(11)	61.5(7)	B(2)–B(11)–C(7)	58.6(11)	58.1(6)
B(6)–B(2)–B(1)	61.1(11)	59.8(6)			

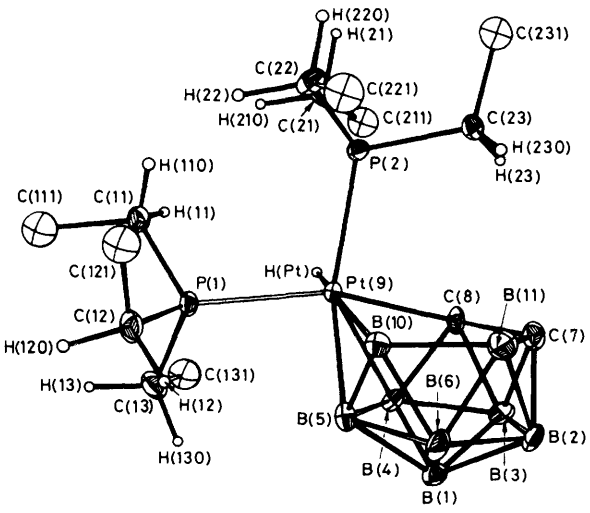

Figure 1. Perspective view of [9-H-9,9-$(Et_3P)_2$-$\mu_{10,11}$-H-7,8,9-$C_2PtB_8H_{10}$] (1). Thermal ellipsoids are constructed at the 30% probability level, except for H atoms which have an artificial radius of 0.1 Å for clarity

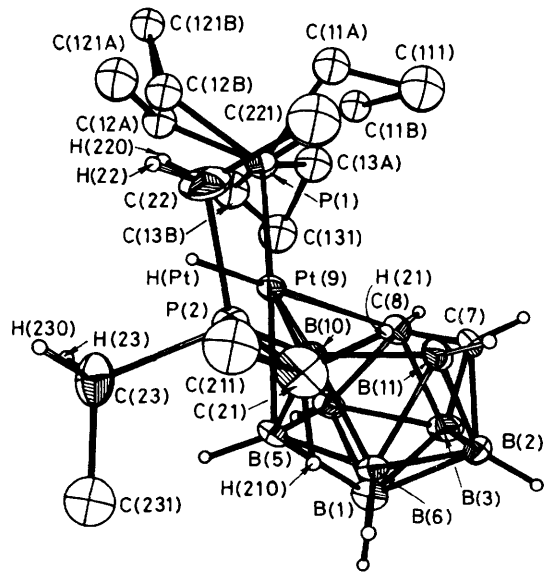

Figure 2. The molecule [9-H-9,10-$(Et_3P)_2$-7,8,9-$C_2PtB_8H_9$] (2), with thermal ellipsoids as in Figure 1

Table 2. Least-squares planes data for [9-H-9,9-$(Et_3P)_2$-$\mu_{10,11}$-H-7,8,9-$C_2PtB_8H_{10}$] (1) and [9-H-9,10-$(Et_3P)_2$-7,8,9-$C_2PtB_8H_9$] (2)

(*a*) Coefficients *P*, *Q*, *R*, and *S* (Å), where the expression $Px + Qy + Rz = S$ defines the plane * (*x*, *y*, and *z* are atomic fractional co-ordinates)

	P	*Q*	*R*	*S*
Plane 1: Compound (1), B(2),B(3),B(4),B(5),B(6)				
	0.748	9.821	3.911	4.085
Plane 2: Compound (1), C(7),C(8),Pt(9),B(10),B(11)				
	0.170	9.963	2.968	2.332
Plane 3: Compound (2), B(2),B(3),B(4),B(5),B(6)				
	8.873	1.359	−11.160	1.793
Plane 4: Compound (2), C(7),C(8),Pt(9),B(10),B(11)				
	8.822	−0.218	−11.658	−0.296

(*b*) Individual atomic deviations (Å) from each plane

Plane 1: B(2) −0.020, B(3) 0.014, B(4) −0.004, B(5) −0.008, B(6) 0.017, B(1) 0.898

Plane 2: C(7) −0.032, C(8) 0.136, Pt(9) −0.144, B(10) 0.156, B(11) −0.116

Plane 3: B(2) −0.083, B(3) 0.083, B(4) −0.052, B(5) 0.005, B(6) 0.047, B(1) 0.935, H(2) 0.269, H(3) 0.507, H(4) 0.392, H(5) 0.436, H(6) 0.640

Plane 4: C(7) −0.065, C(8) 0.186, Pt(9) −0.194, B(10) 0.216, B(11) −0.143, H(7) −0.609, H(8) −0.021, P(2) −0.321, H(11) −0.648

(*c*) Root mean square deviations (Å) of atoms defining each plane from the plane

Plane 1: 0.014	Plane 3: 0.061
Plane 2: 0.125	Plane 4: 0.170

(*d*) Dihedral angles (°)

Plane 1–Plane 2: 4.1	Plane 3–Plane 4: 7.5

* All atoms given unit weights.

Table 3. Polyhedral and *exo*-polyhedral distances (Å) and angles (°) in [9-H-9,9-$(Et_3P)_2$-$\mu_{10,11}$-H-7,8,9-$C_2PtB_8H_{10}$] (1)

Pt(9)–P(1)	2.304(3)	Pt(9)–P(2)	2.364(3)
P(1)–C(11)	1.791(14)	P(2)–C(21)	1.865(13)
P(1)–C(12)	1.825(16)	P(2)–C(22)	1.817(14)
P(1)–C(13)	1.828(17)	P(2)–C(23)	1.818(12)
C(11)–C(111)	1.63(3)	C(21)–C(211)	1.50(3)
C(12)–C(121)	1.58(3)	C(22)–C(221)	1.49(3)
C(13)–C(131)	1.58(3)	C(23)–C(231)	1.55(3)
P(1)–Pt(9)–P(2)	104.0(1)	P(2)–Pt(9)–C(8)	95.9(4)
P(1)–Pt(9)–C(8)	157.6(4)	P(2)–Pt(9)–B(4)	141.3(5)
P(1)–Pt(9)–B(4)	113.1(5)	P(2)–Pt(9)–B(5)	144.9(5)
P(1)–Pt(9)–B(5)	89.3(4)	P(2)–Pt(9)–B(10)	99.8(4)
P(1)–Pt(9)–B(10)	101.6(4)	Pt(9)–P(2)–C(21)	114.6(5)
Pt(9)–P(1)–C(11)	114.4(5)	Pt(9)–P(2)–C(22)	120.6(6)
Pt(9)–P(1)–C(12)	116.5(6)	Pt(9)–P(2)–C(23)	111.2(4)
Pt(9)–P(1)–C(13)	113.7(6)	C(21)–P(2)–C(22)	100.7(7)
C(11)–P(1)–C(12)	105.5(8)	C(21)–P(2)–C(23)	105.0(8)
C(11)–P(1)–C(13)	104.4(8)	C(22)–P(2)–C(23)	103.0(8)
C(12)–P(1)–C(13)	100.9(9)	P(2)–C(21)–C(211)	113.8(13)
P(1)–C(11)–C(111)	114.7(13)	P(2)–C(22)–C(221)	117.9(13)
P(1)–C(12)–C(121)	115.0(13)	P(2)–C(23)–C(231)	114.7(11)
P(1)–C(13)–C(131)	112.4(13)		

angles. There are a number of differences between corresponding parameters that are statistically significant. In terms of χ, the ratio of the change to its standard deviation,* the major differences in bond lengths, mapping (1) ⟶ (2), are reductions in Pt(9)–B(10), $\chi = 8.0$; B(10)–B(11), $\chi = 5.6$; C(7)–C(8), $\chi = 5.4$; B(4)–C(8), $\chi = 4.2$; and B(3)–C(7), $\chi = 3.2$. All other bond length changes have $\chi < 3.0$. Similar analysis of comparable angles reveals significant increases in Pt(9)–B(10)–B(5), $\chi = 7.4$; and B(3)–C(8)–B(4), $\chi = 3.5$; and decreases in Pt(9)–B(5)–B(10), $\chi = 7.1$; C(8)–Pt(9)–B(4), $\chi = 4.9$; B(11)–B(6)–B(10), $\chi = 4.7$; and C(8)–B(3)–B(4), $\chi = 3.7$; no other angle altering by as much as 3.0 σ.

We can interpret the majority of these structural changes in terms of differing *formal* polyhedral geometries for (1) and (2). Although not located in the crystallographic study and not unambiguously detected from the i.r. or n.m.r. spectra, it is likely that a μ-H function lies along the B(10)–B(11) edge of (1).† There are innumerable precedents for B–B edge bridging in an open face, and certainly the B(10)–B(11) distance in (1) exceeds that in (2) by approximately the expected amount, namely 0.143(26) Å. Consistent with its quasi-octahedral geometry, the metal atom of (1) could be formally considered as Pt^{IV}, and thus a source of three electrons to the then 26-electron *nido*-icosahedral cluster.

In (2) the P(2) phosphine ligand has replaced the hydrogen atom previously terminal to B(10), which, therefore, now acts as a three-electron function for cluster bonding. The $\mu_{10,11}$-H atom has also been lost, and the metal atom adopts an essentially planar co-ordination geometry typical of Pt^{II}. The polyhedron has therefore access to only 24 skeletal electrons, and in simple terms would be expected to adopt a *closo*-octadecahedral geometry. Although the actual polyhedral shape is obviously still very open, clear evidence for a distortion from the *nido*-icosahedral architecture of (1) towards a closed structure is revealed by analysis of the structural data. The three most significant angular changes result from displacement of Pt(9) upward out of the open face of (2) into a very distorted quasi-6-connected position.‡ Neither the open face of (1) nor that of (2) is strictly planar but, as detailed in Table 2, the root mean square deviation (r.m.s.d.) of Plane 2 is appreciably less than that of Plane 4 and, as a result of this distortion, the distances Pt(9) · · · C(7) and Pt(9) · · · B(11) are both *ca.* 0.24 Å shorter in (2) than in (1) (2.991 and 3.050 Å *versus* 3.234 and 3.306 Å, respectively). At *ca.* 3 Å, however, the two former connectivities are clearly still non-bonding. Presumably the open framework displayed by (2) is a consequence of the inability of the Pt(H)(PEt_3) fragment to match fully the bonding requirements of the six-atom open face of the $C_2B_8H_9(PEt_3)$ ligand, and is related to the open or 'slipped' structures found when ML_2 fragments (M = Pd or Pt; L = tertiary phosphine or isocyanide) attempt to cap the five- or six-atom open faces of a wide range of carbaborane polyhedra.[7-9] It has recently been argued[10] that the distortions of carbaplatinaboranes of general formula $[(R_3P)_2PtC_2B_xH_xR'_2]$ (R′ = H or Me) from *closo* geometries could be discussed in terms of the donation of four electrons from metal to cage. However, we find herein significant structural differences between the polyhedra of (1) and (2) that are consistent only with a lower

* If *i* and *j* are the parameters compared, $\chi = |i - j|/(\sigma_i^2 + \sigma_j^2)^{\frac{1}{2}}$.

† From measurement of the amount of gas evolved on its pyrolysis, (1) clearly has an excess of two hydrogen atoms relative to (2).

‡ Connectivity numbers are expressed only with respect to the polyhedron. In the *formal* description of the cage of (2) adopting an octadecahedral geometry, Pt(9) occupies the 6-, and C(8) and B(4) the 4-connected positions.

Table 4. Polyhedral distances and phosphine ligand distances (Å) and angles (°) in [9-H-9,10-$(Et_3P)_2$-7,8,9-$C_2PtB_8H_9$] (2)

B(1)–H(1)	1.14(8)	C(7)–H(7)	0.86(8)
B(2)–H(2)	0.95(8)	C(8)–H(8)	0.82(8)
B(3)–H(3)	0.95(9)	Pt(9)–P(1)	2.293(3)
B(4)–H(4)	1.01(9)	B(10)–P(2)	1.914(12)
B(5)–H(5)	1.03(9)	B(11)–H(11)	1.04(9)
B(6)–H(6)	1.17(8)	C(12B)–C(121B)	1.55(4)
P(1)–C(11A)	1.98(2)	C(13A)–C(131)	1.60(3)
P(1)–C(11B)	1.72(3)	C(13B)–C(131)	1.26(4)
P(1)–C(12A)	1.78(2)	P(2)–C(21)	1.797(12)
P(1)–C(12B)	1.89(4)	P(2)–C(22)	1.805(11)
P(1)–C(13A)	1.77(3)	P(2)–C(23)	1.833(13)
P(1)–C(13B)	1.97(4)	C(21)–C(211)	1.570(19)
C(11A)–C(111)	1.38(3)	C(22)–C(221)	1.530(21)
C(11B)–C(111)	1.68(3)	C(23)–C(231)	1.533(18)
C(12A)–C(121A)	1.44(5)		
C(12A)–C(121B)	1.58(3)		

Pt(9)–P(1)–C(11A)	108.8(7)	P(1)–Pt(9)–C(8)	96.6(3)
Pt(9)–P(1)–C(12A)	118.7(7)	P(1)–Pt(9)–B(4)	120.6(3)
Pt(9)–P(1)–C(13A)	119.4(9)	P(1)–Pt(9)–B(5)	167.7(3)
C(11A)–P(1)–C(12A)	105.5(10)	P(1)–Pt(9)–B(10)	146.6(3)
C(11A)–P(1)–C(13A)	97.6(11)	P(2)–B(10)–Pt(9)	117.1(5)
C(12A)–P(1)–C(13A)	104.1(12)	P(2)–B(10)–B(5)	122.1(7)
Pt(9)–P(1)–C(11B)	118.2(9)	P(2)–B(10)–B(6)	117.7(7)
Pt(9)–P(1)–C(12B)	111.1(11)	P(2)–B(10)–B(11)	122.7(8)
Pt(9)–P(1)–C(13B)	112.9(12)	B(10)–P(2)–C(21)	110.6(6)
C(11B)–P(1)–C(12B)	112.5(15)	B(10)–P(2)–C(22)	114.3(6)
C(11B)–P(1)–C(13B)	101.1(15)	B(10)–P(2)–C(23)	114.0(5)
C(12B)–P(1)–C(13B)	99.0(18)	C(21)–P(2)–C(22)	106.0(7)
P(1)–C(11A)–C(111)	112.8(16)	C(21)–P(2)–C(23)	108.0(7)
P(1)–C(12A)–C(121A)	109.8(23)	C(22)–P(2)–C(23)	103.2(7)
P(1)–C(12A)–C(121B)	120.6(17)	P(2)–C(21)–C(211)	115.1(11)
P(1)–C(13A)–C(131)	109.4(17)	P(2)–C(22)–C(221)	111.1(10)
P(1)–C(11B)–C(111)	111.9(17)	P(2)–C(23)–C(231)	114.5(10)
P(1)–C(12B)–C(121B)	115.0(25)		
P(1)–C(13B)–C(131)	115.2(29)		

formal oxidation state for the metal atom in the latter compared with that in the former.

Tables 3 and 4 list molecular parameters involving refined atoms not defining the polyhedral surface, except for angles involving the cage H atoms of (2), which have been deposited. In compound (1) the difference between Pt–P bond lengths is highly significant ($\chi = 14.1$), and is a consequence of the greater *trans* influence of boron over cage carbon in molecules of this type.[11] The *cis*-$Pt(PEt_3)_2$ moiety adopts a local stereochemistry that approximates to that previously[7] termed 'type (i)' but, presumably because of the long Pt(9)–P(2) bond, interligand congestion does not occur. Thus, contacts H(110) · · · H(22) and H(11) · · · H(210) are both >2.4 Å, and the Pt(9)–P(1)–C angles are essentially equivalent. The geometry at P(2) is more distorted, however, with the ethyl function standing above the open face making the narrowest Pt–P–C and the widest C–P–C angles. Closest contacts between its methylene H atoms and facial cage atoms are H(23) · · · C(8) 2.788, H(23) · · · C(7) 3.058, H(230) · · · C(7) 3.082, and H(230) · · · B(11) 3.063 Å.

In (2) the phosphine ligand bound to the metal is seriously disordered, and the model used (see Experimental section) results in six apparent P–C distances, 1.72(3)—1.98(2) Å, and seven apparent C–C distances, 1.26(4)—1.68(3) Å. Angles at P(1) span the range 97.6(11)—119.4(9)°, and at the methylene carbons 109.4(17)—120.6(17)°. Some of the bond lengths here are clearly unrealistic, and possibly a better approximation to the electron density distribution could have been found. However, the cost would be an inferior data : variable ratio, and considerably more computational time, and since the *important* part of the overall structure, *i.e.* the polyhedron, is fairly accurately defined, optimisation of the P(1) ligand was not pursued.

Figures 3 and 4 of the Supplementary data present views of the crystal structures of (1) and (2) projected onto, respectively, the (0 1 0) and (1 0 0) crystal faces. In neither array are there any serious intermolecular contacts.

The formation of compound (1), and its subsequent pyrolysis to generate (2) are in marked contrast to other studies of the insertion of nucleophilic metal fragments into *nido*-carbaboranes. Thus $[Co(PEt_3)_4]$ reacts with *nido*-5,6-$C_2B_8H_{12}$ or *nido*-4,5-$C_2B_7H_{11}$ spontaneously to eliminate one mol equiv. of H_2 and generate *closo*-carbacobaltaboranes directly.[11] There is a growing body of evidence[12] to support the idea that the reactivities of cobalt and nickel sub-group nucleophiles towards a wide variety of carbaboranes are markedly different.

Perhaps more directly relevant to the results described herein is our previous observation[5] that a $Pt(PEt_3)_2$ fragment inserts into one μ-B–H–B function of *nido*-2,3-$C_2B_4H_4R_2$ (R = H or Me) to afford isolable, non-expanded, *nido* species with a bridging *trans*-$PtH(PEt_3)_2$ unit. On heating to 100 °C in hexane, these compounds release H_2 yielding *closo* products[7] *via* mechanisms that are not well understood, since for R = Me, cage carbon atom adjacency is maintained, whereas for R = H it is not. We have speculated[7] on the possibility that the hydrogen atoms lost as H_2 are coupled from mutually *cis* co-ordination sites on platinum in a transition state.

It is possible that compound (1) is formed by an analogous initial oxidative insertion of a $Pt(PEt_3)_2$ fragment into one of the μ-B–H–B functions of *nido*-5,6-$C_2B_8H_{12}$, which is followed by interaction of the resulting platinum(II) centre with a cage carbon atom. However, the next stage in the pyrolytic formation of (2) is more unusual, although migration of a triphenylphosphine ligand from nickel to a boron atom has been reported[13] on thermolysis of *closo*-[3,3-$(Ph_3P)_2$-3,1,2-$NiC_2B_9H_{11}$]. If we examine the illustration of the open polyhedral face of (1) shown in the Scheme then it can be seen that if we assume that dissociative loss of one of

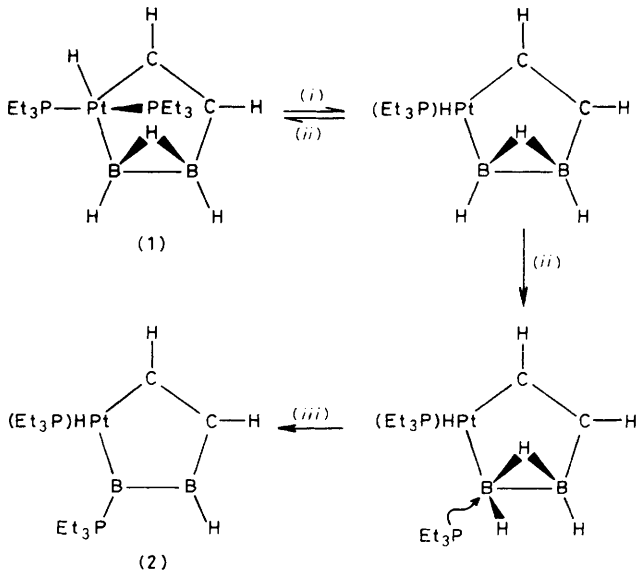

Scheme. (*i*) $-PEt_3$, the loss of a particular phosphine is not implied; (*ii*) $+PEt_3$; (*iii*) $-H_2$

the two triethylphosphine ligands occurs then the free phosphine can now attack the adjacent boron centre resulting in a concerted loss of molecular hydrogen. Clearly such a scheme provides only a broad outline of what is happening, and questions such as which phosphine ligand dissociates, and the exact nature of the hydrogen elimination step remain to be resolved. Thus, there is also the possibility, although we consider it less likely, that the μ-B–H–B hydrogen becomes bonded to the platinum, with an implied oxidative-addition ($Pt^{II} \longrightarrow Pt^{IV}$) prior to loss of molecular hydrogen.

Experimental

Nuclear magnetic resonance spectra were recorded on JEOL FX 90Q, PS 100, and FX 200 spectrometers. Chemical shifts are relative to $SiMe_4$ (^1H), 85% H_3PO_4 (external) (^{31}P), and $BF_3{\cdot}OEt_2$ (external) (^{11}B); positive values representing shifts to high frequency of the reference. I.r. spectra were measured as Nujol mulls on a Perkin-Elmer 457 spectrophotometer. Melting points were measured in sealed, evacuated tubes. All experiments were carried out under dry, oxygen-free nitrogen using Schlenk tube techniques. Solvents were dried and distilled under nitrogen before use. The compounds $[Pt_2(\mu\text{-cod})(PEt_3)_4]$ [5] and *nido*-5,6-$C_2B_8H_{12}$ [14] were prepared by literature methods.

Synthesis of [9-H-9,9-$(Et_3P)_2$-$\mu_{10,11}$-H-7,8,9-$C_2PtB_8H_{10}$] (1).—A solution of $[Pt_2(\mu\text{-cod})(PEt_3)_4]$ (0.24 g, 0.25 mmol) in diethyl ether (5 cm^3) was added dropwise *via* a syringe to a solution of *nido*-5,6-$C_2B_8H_{12}$ (0.06 g, 0.5 mmol) in diethyl ether (5 cm^3) at room temperature. The resulting pale brown solution was evaporated to dryness under vacuum, and the tan coloured residue recrystallised from tetrahydrofuran–diethyl ether (1 : 5) at −20 °C. Pale yellow *crystals* of [9-H-9,9-$(Et_3P)_2$-$\mu_{10,11}$-H-7,8,9-$C_2PtB_8H_{10}$] (1) were obtained (0.19 g, 70%) (Found: C, 30.4; H, 8.2. $C_{14}H_{42}B_8P_2Pt$ requires C, 30.3; H, 7.6%); m.p. 104—106 °C; $\nu_{max.}$ at 2 555s (BH), 2 520vs (BH), 2 494s (BH), 2 010s (PtH), 1 413m, 1 207w, 1 162w, 1 075w, 1 030s, 1 015m, 969w, 946vw, 915w, 902vw, 888vw, 870w, 759s, 722m, 710w, 680vw, 660vw, 643w, and 630w cm^{-1}. N.m.r. spectra: ^1H (C_6D_6, 25 °C), δ 3.29 (br, s, 1 H, cage CH), 2.82 (br, s, 1 H, cage CH), 1.60 (m, 12 H, PCH_2CH_3), 0.80 (m, 18 H, PCH_2CH_3), −3.5, −4.4, −8.1, and −11.9 (br, s, cage BH, BHB, and PtH); ^{31}P-{^1H} ($CD_3C_6D_5$, −80 °C), δ 3.9 [d, J(PtP) 2 335, J(PP) 22] and −7.2 p.p.m. [d, J(PtP) 2 349, J(PP) 22 Hz]; ^{31}P-{PEt_3 protons selectively decoupled} ($CD_3C_6D_5$, −80 °C), δ 3.9 [d, J(PtP) 2 335, J(PP) 22] and −7.2 p.p.m. [t, J(PtP) 2 327, J(PP) 22, J(PH) 22 Hz]; ^{11}B-{^1H} (C_6D_6, 25 °C), δ 8.9 (2 B), −11.9 (2 B), −22.2 and −26.8 (4 B) p.p.m.

Pyrolysis of (1).—A solution of (1) (0.28 g, 0.5 mmol) in toluene (10 cm^3) was transferred to a tube fitted with a Westef high-pressure stopcock. The tube was cooled to −196 °C, evacuated, sealed and allowed to warm to room temperature before being placed in an oven set at 100 °C. After *ca.* 1 h the tube was cooled to −196 °C and opened to the vacuum line. A non-condensable gas (0.5 mmol) was removed and the deep red solution then allowed to warm to room temperature before being evaporated to dryness under vacuum. The red residue was extracted with diethyl ether (5 cm^3) and cooled to −20 °C. Red *crystals* of [9-H-9,10-$(Et_3P)_2$-7,8,9-$C_2PtB_8H_9$] (2) were obtained (0.23 g, 80%) (Found: C, 31.0; H, 8.1. $C_{14}H_{40}B_8P_2Pt$ requires C, 30.3; H, 7.6%); m.p. 116 °C; $\nu_{max.}$ at 2 560m (BH), 2 514s (BH), 2 480sh (BH), 2 465m (BH), 2 115m (PtH), 1 408m, 1 256m, 1 040s, 1 010m, 944w, 914vw, 902w, 860w, 842w, 806m, 768s, 753m, 734m, 702w, 697w, 678vw, 662vw, and 640w cm^{-1}. N.m.r. spectra: ^1H (C_6D_6, 25 °C), δ 3.75 (br, s, 1 H, cage CH), 3.15 (br, s, 1 H, cage CH), 2.2—1.7 (m, 12 H, PCH_2CH_3), 1.3—0.9 (m, 18 H, PCH_2CH_3), −17.5 [d of d, PtH, J(PH) 24 and 16, J(PtH) 600 Hz]; ^{31}P-{^1H} ($CD_3C_6D_5$, −70 °C), δ 17.2 [s, J(PtP) 2 775] and 9.6 p.p.m. [J(PtP) 95 Hz]; ^{11}B-{^1H} (C_6D_6, 25 °C), δ 9.4 [s, 1 B, J(PtB) 275], 8.9 (s, 1 B), 4.8 [s, 1 B, J(PtB) 261], −0.5 (s, 1 B), −14.2 [s, 1 B, J(PtB) 387], −14.9 [d, 1 B, J(PB) 122], −21.8 (s, 1 B), and −24.4 p.p.m. [s, 1 B, J(PtB) 326 Hz].

Molecular Structure Determinations of (1) *and* (2).—Experimental conditions were generally similar for both determinations, and are, therefore, described for (1) only, data in brackets representing differences with respect to compound (2).

A single crystal, *ca.* 0.025 × 0.025 × 0.03 cm (0.02 × 0.03 × 0.045 cm) was secured inside a subsequently sealed 0.05 cm Lindemann tube under an atmosphere of dry nitrogen. Oscillation and zero and first-level (equi-inclination) Weissenberg photographs (Cu-K_α X-radiation) yielded approximate cell dimensions, and indicated the space group to be either $P2_12_12$ or $P2_12_12_1$ (unambiguously $P2_1/c$) from available systematic absences.

On transference to an Enraf-Nonius CAD4 diffractometer operating with graphite-monochromated Mo-K_α X-radiation (λ_{α_1} = 0.709 26, λ_{α_2} = 0.713 54 Å), accurate cell parameters were obtained from least-squares refinement of 25 strong general reflections in the range 16 (15) < θ < 17°. Three-dimensional intensity data were recorded with the same crystal on the same instrument at 293 K, using ω–2θ scans in 96 steps, in the range $1.5 \leqslant \theta \leqslant 30.0$ (25.0)°. Scan widths were given by $S = A + B\tan\theta$ with $A = 0.9$ (0.8) and $B = 0.15$. After a rapid prescan only those reflections considered significantly intense [$I \geqslant 2.0(I)$] were rescanned such that the final net intensity had $I \geqslant 33\sigma(I)$, subject to a maximum measuring time of 90 (60) s.

Two orientation and two intensity control reflections were re-monitored every 100 reflections and 3 600 s respectively, but for neither compound was any crystal movement or decay, or source variance detectable over the *ca.* 67 (52) h of X-ray exposure. Of 3 918 unique reflections, $+h + k + l$ (4 296, $\pm h + k + l$), corrected for X-ray absorption and for Lorentz and polarisation effects, 3 303 (3 194) with $F \geqslant 2.0\sigma(F)$ were retained for structure solution and refinement.

Crystal data for (1). $C_{14}H_{42}B_8P_2Pt$, M = 554.0, Orthorhombic, a = 14.825(4), b = 10.1367(13), c = 16.1193(15) Å, U = 2 422.4 $Å^3$, D_m not measured, Z = 4, D_c = 1.519 g cm^{-3}, $F(000)$ = 1 096, μ(Mo-$K_{\bar{\alpha}}$) = 58.6 cm^{-1}. Space group $P2_12_12_1$ (D_2^4, no. 19) from systematic absences.

Crystal data for (2). $C_{14}H_{40}B_8P_2Pt$, M = 551.98, Monoclinic, a = 9.7813(16), b = 12.312(3), c = 20.519(3) Å, β = 99.053(16)°, U = 2 440.2 $Å^3$, D_m not measured, Z = 4, D_c = 1.503 g cm^{-3}, $F(000)$ = 1 088, μ(Mo-$K_{\bar{\alpha}}$) = 56.4 cm^{-1}, space group $P2_1/c$ (C_{2h}^5, no. 14) from systematic absences.

Both structures were solved by conventional methods, Patterson syntheses yielding metal positions and difference-Fourier maps all other non-hydrogen atoms, and were refined by full-matrix least-squares methods. Cage carbon atoms were identified on the basis of internuclear separations and refined (as boron) thermal parameters. For (1), parallel refinement of the enantiomeric model resulted in a significantly poorer R factor and higher atomic estimated standard deviations, and was, therefore, rejected. Structure factors were weighted according to $w = [\sigma^2(F_o) + Q(F_o)^2]^{-1}$ with Q = 0.002 055 (0.000 928).

In the final stages of refinement Pt, P, B, and methylene C

Table 5. Fractional atomic co-ordinates ($\times 10^5$ for Pt and P, $\times 10^4$ for B and C) of refined atoms in [9-H-9,9-$(Et_3P)_2$-$\mu_{10,11}$-H-7,8,9-$C_2PtB_8H_{10}$] (1)

Atom	*x*	*y*	*z*	Atom	*x*	*y*	*z*
B(1)	1 850(14)	4 183(15)	1 885(10)	C(11)	1 004(14)	2 087(18)	−1 796(8)
B(2)	2 180(17)	2 945(19)	2 583(9)	C(12)	2 707(12)	3 179(20)	−1 285(10)
B(3)	1 048(16)	3 161(16)	2 343(10)	C(13)	1 116(12)	4 657(15)	−1 074(11)
B(4)	973(13)	3 573(18)	1 279(9)	C(21)	167(10)	−744(14)	−494(11)
B(5)	2 119(12)	3 645(17)	866(9)	C(22)	2 067(10)	−1 060(17)	−514(9)
B(6)	2 861(13)	3 272(18)	1 725(9)	C(23)	1 171(14)	−1 140(13)	1 046(8)
C(7)	1 557(13)	1 598(15)	2 296(9)	C(111)	1 118(17)	2 764(24)	−2 710(14)
C(8)	848(9)	1 989(14)	1 591(7)	C(121)	3 214(15)	1 859(23)	−1 524(15)
Pt(9)	12 961(3)	20 761(4)	3 289(2)	C(131)	69(15)	4 760(24)	−916(15)
B(10)	2 725(10)	2 183(16)	900(9)	C(211)	−697(15)	−427(23)	−52(15)
B(11)	2 617(14)	1 598(18)	1 954(12)	C(221)	2 983(15)	−1 172(25)	−138(15)
P(1)	15 344(23)	29 701(38)	−9 666(19)	C(231)	999(14)	−2 636(20)	944(12)
P(2)	11 984(23)	−2 173(27)	790(17)				

Table 6. Fractional atomic co-ordinates ($\times 10^5$ for Pt and P, $\times 10^4$ for B and C, $\times 10^3$ for H) of refined atoms in [9-H-9,10-$(Et_3P)_2$-7,8,9-$C_2PtB_8H_9$] (2) [a]

Atom	*x*	*y*	*z*	Atom	*x*	*y*	*z*
B(1)	3 372(12)	3 460(11)	659(5)	C(121B) [d]	−3 648(25)	−293(20)	524(12)
B(2)	2 745(12)	4 458(10)	1 194(7)	C(13A) [b]	−2 568(27)	2 161(22)	−207(14)
B(3)	1 938(12)	4 277(11)	381(7)	C(13B) [c]	−2 086(39)	1 150(35)	−455(21)
B(4)	1 818(12)	2 847(10)	232(6)	C(131)	−1 827(21)	1 908(15)	−831(10)
B(5)	2 910(11)	2 174(9)	968(5)	C(21)	3 484(15)	2 146(12)	3 106(5)
B(6)	3 483(10)	3 264(9)	1 519(5)	C(211)	3 829(16)	1 457(13)	3 754(8)
C(7)	1 029(9)	4 248(8)	1 009(5)	C(22)	993(13)	921(11)	2 693(17)
C(8)	579(10)	3 487(8)	468(6)	C(221)	77(20)	1 847(15)	2 872(10)
Pt(9)	6 105(3)	18 502(3)	8 482(2)	C(23)	3 486(15)	207(10)	2 273(6)
B(10)	2 165(10)	2 379(9)	1 663(5)	C(231)	4 995(16)	402(14)	2 186(8)
B(11)	1 876(11)	3 706(10)	1 727(6)	H(1)	431(8)	356(7)	40(4)
P(1)	−16 829(30)	14 768(28)	4 937(19)	H(2)	312(8)	517(7)	127(4)
P(2)	25 264(29)	14 414(25)	24 138(13)	H(3)	190(8)	480(7)	4(4)
C(11A) [b]	−2 780(23)	2 051(18)	1 147(12)	H(4)	179(8)	253(7)	−22(5)
C(11B) [c]	−2 875(27)	2 482(23)	559(14)	H(5)	338(8)	146(7)	87(4)
C(111)	−2 535(20)	3 138(15)	1 283(10)	H(6)	457(8)	326(6)	185(4)
C(12A) [b]	−2 202(22)	101(19)	368(12)	H(7)	57(8)	480(7)	111(4)
C(12B) [c]	−2 192(38)	128(32)	829(21)	H(8)	0(8)	379(7)	20(4)
C(121A) [d]	−2 077(38)	−450(33)	990(19)	H(11)	191(8)	411(7)	218(5)

[a] All population parameters 1.0, except where indicated otherwise (see text). [b] Population 0.5833. [c] Population 0.4167. [d] Population 0.5.

atoms were allowed anisotropic motion,* methyl carbons were refined isotropically, and methylene and platinum-bound H atoms were included in idealised positions, Pt–H 1.50, C–H 1.08 Å [for (1) $U_H = 0.07$ Å^2; for (2) $U_{CH_2} = 0.10$ Å^2, $U_{PtH} = 0.06$ Å^2]. Only for (2) could terminal cage H atoms be located, and these were subsequently refined with invariant thermal parameters ($U = 0.06$ Å^2).

Refinement was cycled to convergence, $R = 0.0575$, $R' = 0.0611$ ($R = 0.0578$, $R' = 0.0552$), for 196 (224) variables. In a final ΔF synthesis, no peak greater than 1.2 (1.1) e Å^{-3} or trough less than −1.1 (−0.9) e Å^{-3} occurred, and there was no unusual systematic variation of the r.m.s.d. of a reflection of unit weight *versus* parity group, $(\sin\theta)/\lambda$, F_o, *h*, *k*, or *l*. All crystallographic calculations employed programs of the SHELX 76 system [15] implemented on the University of London Computer Centre CDC 7600 computer. Coefficients for analytical approximations to the atomic scattering factors were taken from ref. 16. Tables 5 and 6 list the derived fractional co-ordinates of refined atoms in compounds (1) and (2). Least-squares planes were analysed by the program XANADU,[17] and Figures were constructed using ORTEP-II.[18]

* For (2) the phosphine ligand bound to the metal atom is rather complexly disordered, and has been modelled in terms of two sets of (isotropically refined) methylene carbon atoms of site occupancy factors 0.5833 (type A) and 0.4167 (type B), and two complete, C(111) and C(131), and two half, C(121A), C(121B), methyl carbons. No hydrogen atoms were assigned to this ligand in the crystallographic study.

Acknowledgements

We thank the S.E.R.C. for support, Dr. M. B. Hursthouse for use of the diffractometer, and Macalester College, St. Paul, Minnesota, for study leave (to W. C. W.).

References

1 Part 12, G. K. Barker, M. P. Garcia, M. Green, F. G. A. Stone, and A. J. Welch, *J. Chem. Soc., Dalton Trans.*, 1982, 1679.
2 M. Green, J. L. Spencer, and F. G. A. Stone, *J. Chem. Soc., Dalton Trans.*, 1979, 1679.
3 See, for example, R. B. Maynard, E. Sinn, and R. N. Grimes, *Inorg. Chem.*, 1981, **20**, 1201; M. J. Calhorda, D. M. P. Mingos, and A. J. Welch, *J. Organomet. Chem.*, 1982, **228**, 309; D. N. Cox, D. M. P. Mingos, and R. Hoffmann, *J. Chem. Soc., Dalton Trans.*, 1981, 1788; M. E. O'Neill and K. Wade, *Inorg. Chem.*, 1982, **21**, 461; and refs. therein.
4 For example, C. W. Jung, R. T. Baker, and M. F. Hawthorne, *J. Am. Chem. Soc.*, 1981, **103**, 810.

5 G. K. Barker, M. Green, F. G. A. Stone, A. J. Welch, T. P. Onak, and G. Siwapanyoyos, *J. Chem. Soc., Dalton Trans.*, 1979, 1687.
6 G. K. Barker, M. Green, F. G. A. Stone, A. J. Welch, and W. C. Wolsey, *J. Chem. Soc., Chem. Commun.*, 1980, 627.
7 G. K. Barker, M. Green, F. G. A. Stone, and A. J. Welch, *J. Chem. Soc., Dalton Trans.*, 1980, 1186.
8 G. K. Barker, M. Green, J. L. Spencer, F. G. A. Stone, B. F. Taylor, and A. J. Welch, *J. Chem. Soc., Chem. Commun.*, 1975, 804.
9 W. E. Carroll, M. Green, F. G. A. Stone, and A. J. Welch, *J. Chem. Soc., Dalton Trans.*, 1975, 2263; A. J. Welch, *ibid.*, 1975, 2270; 1977, 962; D. M. P. Mingos, M. I. Forsyth, and A. J. Welch, *ibid.*, 1978, 1363; D. M. P. Mingos and A. J. Welch, *ibid.*, 1980, 1674.
10 S. K. Boocock, N. N. Greenwood, M. J. Hails, J. D. Kennedy, and W. S. McDonald, *J. Chem. Soc., Dalton Trans.*, 1981, 1415.
11 G. K. Barker, M. P. Garcia, M. Green, G. N. Pain, F. G. A. Stone, S. K. R. Jones, and A. J. Welch, *J. Chem. Soc., Chem. Commun.*, 1981, 652 and refs. therein.
12 G. K. Barker, M. P. Garcia, M. Green, F. G. A. Stone, and A. J. Welch, *J. Chem. Soc., Chem. Commun.*, 1983, 137.
13 S. B. Miller and M. F. Hawthorne, *J. Chem. Soc., Chem. Commun.*, 1976, 1786.
14 H. M. Colquhoun, T. J. Greenhough, M. G. H. Wallbridge, S. Hermánek, and J. Plešek, *J. Chem. Soc., Dalton Trans.*, 1978, 944.
15 G. M. Sheldrick, 'SHELX 76,' University Chemical Laboratory, Cambridge, 1976.
16 'International Tables for *X*-Ray Crystallography,' Kynoch Press, Birmingham, 1974, vol. 4.
17 G. M. Sheldrick and P. Roberts, 'XANADU,' University Chemical Laboratory, Cambridge, 1976.
18 C. K. Johnson, 'ORTEP-II,' Report ORNL-5138, Oak Ridge National Laboratory, Tennessee, 1976.

Received 20*th December* 1982; *Paper* 2/2119